

[Home](#) [Search](#) [Collections](#) [Journals](#) [About](#) [Contact us](#) [My IOPscience](#)

## Target electron ionization in $\text{Li}^{2+}$ -Li collisions: A multi-electron perspective

This content has been downloaded from IOPscience. Please scroll down to see the full text.

2015 J. Phys.: Conf. Ser. 601 012010

(<http://iopscience.iop.org/1742-6596/601/1/012010>)

View [the table of contents for this issue](#), or go to the [journal homepage](#) for more

Download details:

IP Address: 193.6.177.68

This content was downloaded on 17/11/2015 at 13:21

Please note that [terms and conditions apply](#).

# Target electron ionization in $\text{Li}^{2+}$ -Li collisions: A multi-electron perspective

M. D. Śpiewanowski<sup>1</sup>, L. Gulyás<sup>2</sup>, M. Horbatsch<sup>1</sup>, J. Goullon<sup>3</sup>,  
N. Ferreira<sup>3</sup>, R. Hubele<sup>3</sup>, V. L. B. de Jesus<sup>4</sup>, H. Lindenblatt<sup>3</sup>,  
K. Schneider<sup>3</sup>, M. Schulz<sup>5</sup>, M. Schuricke<sup>3</sup>, Z. Song<sup>3</sup>, S. Zhang<sup>3</sup>,  
D. Fischer<sup>3</sup>, T. Kirchner<sup>1</sup>

<sup>1</sup>Department of Physics and Astronomy, York University, Toronto, Ontario, Canada M3J 1P3

<sup>2</sup>Institute for Nuclear Research, Hungarian Academy of Sciences (ATOMKI), P.O. Box 51, H-4001 Debrecen, Hungary

<sup>3</sup>Max Planck Institute for Nuclear Physics, Saupfercheckweg 1, 69117 Heidelberg, Germany

<sup>4</sup>Instituto Federal de Educação, Ciência e Tecnologia do Rio de Janeiro (IFRJ), Rua Lucio Tavares 1045, 26530-060 Nilópolis/RJ, Brazil

<sup>5</sup>Department of Physics and LAMOR, Missouri University of Science & Technology, Rolla, Missouri 65409, USA

**Abstract.** Target electron removal in  $\text{Li}^{2+}$ -Li collisions at 2290 keV/amu is studied experimentally and theoretically for ground and excited lithium target configurations. It is shown that in outer-shell ionization a single-electron process plays the dominant part. However, the K-shell ionization results are more difficult to interpret. According to our calculations, the process is shown to be strongly single-particle like. On one hand, a high resemblance between theoretical single-particle ionization and exclusive inner-shell ionization is demonstrated, and contributions from multi-electron processes are found to be weak. On the other hand, it is indicated by the discrepancy between experimental and single-particle theoretical results that multi-electron processes involving ionization from the outer-shell may play a crucial role.

## 1. Introduction

Electron removal from few-electron atoms by fast ions has been of interest to collision physics for many decades [1]. The great interest for these collision systems is mostly fueled by a desire for a better understanding of single- and multi-electron processes. Nevertheless, technical difficulties led to an emphasis on helium atoms among a number of possible simple few-electron atomic targets. Only recently, with the experimental development of the magneto-optical trap reaction-microscope (MOTReMi) setup [2] did it become possible to investigate a whole new range of collision systems allowing to study single- and multi-electron processes with great accuracy. The MOTReMi approach is suitable for alkalis, and lithium has become experimentally accessible as a target atom [2], raising substantial experimental and theoretical interest [3, 4, 5, 6, 7].

In this paper we investigate target ionization in  $\text{Li}^{2+}$ -Li collisions at 2290 keV/amu for  $\text{Li}(1s^22s)$  (ground) and  $\text{Li}(1s^22p)$  (excited) target configurations. We present measurements of single-differential cross sections (SDCS) and investigate single- and multi-particle processes that contribute to  $1s$ ,  $2s$ , and  $2p$  vacancy production. The paper is organized as follows. In Sec. 2.1 we introduce details of the MOTReMi experiment. Theoretical details on the solution



of the time-dependent Schrödinger equation (TDSE) with various approximations and how to incorporate multi-electron effects into a single-particle model are briefly discussed in Sec. 2.2. Section 3 provides experimental and theoretical results and their discussion. Conclusions are presented in Sec. 4.

## 2. Methods

### 2.1. Experimental methods

The experiment was performed using a MOTReMi [2, 8] in the ion storage ring TSR at the Max Planck Institute for Nuclear Physics in Heidelberg.  $\text{Li}^{2+}$  ions were accelerated by a tandem accelerator and stored in the TSR in bunches of about 2 ns duration. The lithium target cloud was laser-cooled to about 2 mK in a MOT. Recoil ions and electrons produced in ionizing collisions were extracted by electric and magnetic fields towards position and time sensitive detectors in a ReMi [9]. While for the recoil ions the final momenta were typically much smaller than the spectrometer acceptance, electrons could only be collected for transverse momenta smaller than 1.9 a.u.

Due to the interaction of the atoms with the cooling lasers, a certain fraction of the target atoms (approximately 20%) is initially in an excited  $1s^22p$  configuration. This made it possible to simultaneously measure cross sections for ionization from the ground state and from the excited state configuration. This is achieved by periodically switching the cooling lasers on and off. During the period with the lasers being switched off 100% of the target state population is in the ground state. During the remaining time a fraction of about 20% of the atoms is in the excited  $1s^22p$  state. Cross sections for the ionization from the excited state are obtained by subtracting the spectra acquired during the two different time periods from each other [3, 8]. It should be noted, that the Zeeman splitting of the atoms in the spectrometer magnetic field (whose orientation nearly coincides with the projectile beam direction) results in the polarization of the  $2p$  state and about 85% of the excited atoms populate the magnetic sub-level with  $m_L = -1$  [8].

Vacancy production in the target K-shell was distinguished from valence vacancy production due to different energy losses  $E_p^{\text{loss}}$  of the projectile for both channels.  $E_p^{\text{loss}}$ , in turn, is given by  $(p_{elz} + p_{recz})v_p$  [9], where  $p_{elz}$  and  $p_{recz}$  are the longitudinal electron and recoil-ion momentum components, respectively, and  $v_p$  is the projectile speed. In the present experiment, the longitudinal electron- and recoil-ion momentum resolutions translate into an energy loss resolution of 30eV (FWHM) which is significantly smaller than the difference between the energy losses for K-shell and valence vacancy production (approximately 65 eV).

### 2.2. Theoretical methods

Our objective is to solve the Schrödinger equation for  $\text{Li}^{2+}$ -Li collisions with the target in ground and excited configurations. Since the full solution to this multi-electron problem is beyond the reach of the state-of-the-art methods used in collision physics, we apply a series of approximations. First, we employ the semi-classical approximation (SCA), where we assume that the projectile is treated as a particle moving along a classical trajectory. This leaves us with a many-electron TDSE in order to deal with the electronic degrees of freedom. Secondly, the projectile electron is frozen, hence, its only influence on the process is assumed to be an additional potential, which screens the nuclear charge and is obtained from a  $1s$ -like charge distribution. In a third step, we reduce the Hamiltonian to a set of one-body operators neglecting the full account of electron-electron interactions, i.e., the independent electron (IEL) model is employed. The effective potential that represents the interactions in the target Li atom is approximated by the exchange-only optimized potential method (OPM) of density functional theory [10]. For more details see [7]. We note that the same potential is used to define the ground and excited states of the target atom. No significant changes are expected by taking the proper effective potential for the excited-state lithium atom due to the tight binding of the inner electrons.

**Table 1.** Single-particle total cross sections for  $\text{He}^{2+}$ -Li and  $\text{Li}^{2+}$ -Li collisions at 2290 keV/amu for  $1s$ ,  $2s$ , and  $2p$  initial states relevant for ground and excited target configurations (in units of  $a_0^2$ , where  $a_0$  is the Bohr radius).

Projectile	Method	Li( $1s$ )	Li( $2s$ )	Li( $2p_{m=0}$ )	Li( $2p_{ m =1}$ )
$\text{He}^{2+}$	CDW-EIS	0.32	2.08	4.33	4.93
	TC-BGM	0.35	2.17	5.58	6.01
$\text{Li}^{2+}$	TC-BGM	0.47	2.30	6.06	6.52

Single-particle TDSEs are solved using the two-center basis generator method (TC-BGM) with a basis that consists of  $1s - 4f$  target states, and  $1s - 4f$  projectile states together with 71 BGM pseudostates [11]. The projectile states are obtained by solving the time independent Schrödinger equation with the following Hamiltonian (in atomic units,  $\hbar = m_e = e = 1$ )

$$H = -\frac{1}{2}\Delta - \frac{Z}{r} + \frac{1}{r} \left(1 - (1 + Zr)e^{-2Zr}\right), \quad (1)$$

where  $r$  denotes the distance between the projectile nucleus and the (passive) electron and  $Z = 3$ . The last term originates from freezing the projectile electron in the  $1s$  state. All basis states are endowed with electron translation factors to ensure Galilean invariance.

Within the single-active electron (SAE) model one simply takes the single-particle solutions for a given initial state (multiplied by two in the case of the doubly occupied  $1s$  orbital) as the final results. To include multi-electron phenomena into the method consistently with the IEL model, we turn to a determinantal analysis [12]. In short, the solutions to the single-particle TDSEs are assembled to form a Slater determinant which is projected onto the final-state determinants. The transition probabilities of interest are thus obtained from combinations of determinants constructed from one-particle density matrix elements, as described in [7].

Extracting electron-emission-energy differential information from TC-BGM solutions is a difficult task. Therefore, we calculate continuum distorted-wave eikonal initial-state (CDW-EIS) single-electron probabilities for inner- and outer-shell ionization using the same target Hamiltonian as in the TC-BGM calculations. Moreover, we restrict our CDW-EIS calculations to the  $\text{He}^{2+}$ -Li collision system, neglecting the influence of the residual electron in the  $\text{Li}^{2+}$  projectile. Hence, our SDCSs for multi-electron processes are calculated by combining TC-BGM probabilities for excitations with doubly-differential cross sections obtained from the CDW-EIS model.

The validity of this approach is confirmed by table 1, where the single-particle total cross sections (TCS) for  $\text{He}^{2+}$ -Li collisions obtained with CDW-EIS are compared with those for  $\text{He}^{2+}$ -Li and  $\text{Li}^{2+}$ -Li collisions obtained with TC-BGM. The single-particle TCSs for ionization in  $\text{He}^{2+}$ -Li collisions for both methods are in good agreement, the differences are within 10% for both inner- and outer-shell ionization of the ground state. The agreement for outer-shell ionization of the excited-state target is not that good and the difference is around 20%. As expected, the situation is slightly worse when comparing  $\text{He}^{2+}$ -Li collision results with  $\text{Li}^{2+}$ -Li data, due to the additional interaction that originates from the presence of the projectile electron.

To understand the origin of the discrepancies between different single-particle TCSs in table 1, we compare in figure 1 ionization probabilities for these collision systems obtained from the CDW-EIS and TC-BGM approaches. The  $1s$  ionization probability curves for  $\text{He}^{2+}$ -Li collisions obtained with both methods fall almost on top of each other (see figure 1 (a)) yielding similar

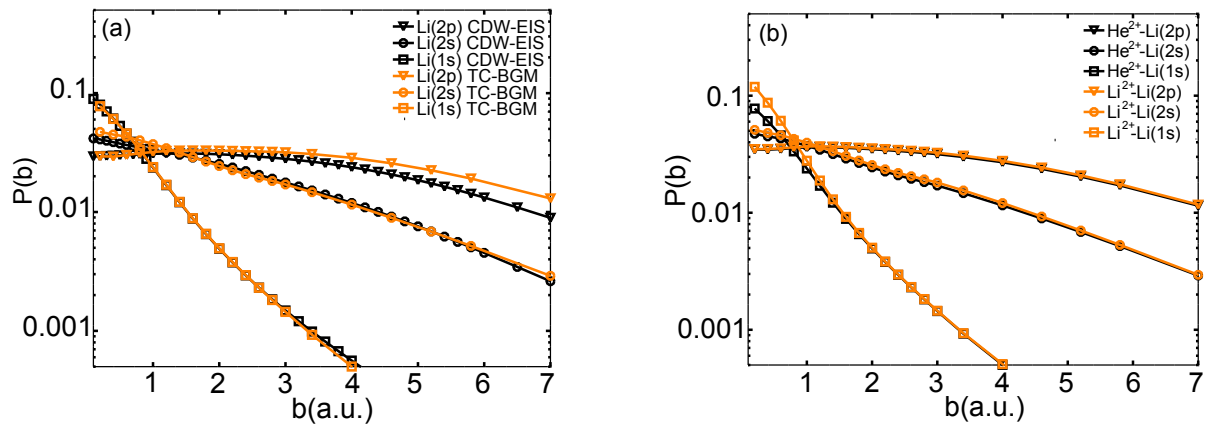


**Figure 1.** Inner- and outer-shell ionization probabilities in  $\text{He}^{2+}$ -Li( $1s^22s$ ),  $\text{He}^{2+}$ -Li( $1s^22p$ ),  $\text{Li}^{2+}$ -Li( $1s^22s$ ), and  $\text{Li}^{2+}$ -Li( $1s^22p$ ) collisions at 2290 keV/amu. (a) Comparison of TC-BGM and CDW-EIS results for  $\text{He}^{2+}$ -Li( $1s^22s$ ) and  $\text{He}^{2+}$ -Li( $1s^22p$ ) collisions. (b) Comparison of TC-BGM results for  $\text{Li}^{2+}$ -Li( $1s^22s$ ) and  $\text{Li}^{2+}$ -Li( $1s^22p$ ) collisions and TC-BGM results for  $\text{He}^{2+}$ -Li( $1s^22s$ ) and  $\text{He}^{2+}$ -Li( $1s^22p$ ) collisions.

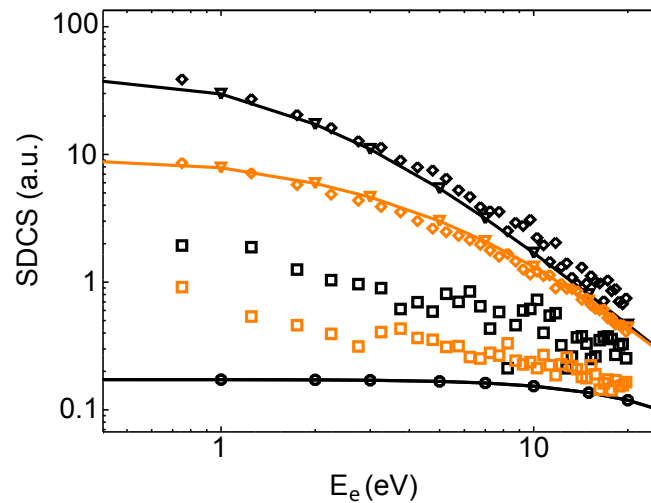
single-particle TCSs. A small difference in ionization from  $2s$  can be seen for low values of the impact parameter. It is also clear from the figure that the CDW-EIS method underestimates the ionization probability from the  $2p$  state for the whole impact-parameter range, as compared to TC-BGM results. For the  $2p$  state we assumed an  $m$  level distribution in accord with the experiment, i.e.,  $|m| = 1$  is populated with 85% and  $m = 0$  with 15%. This procedure is adopted for the results that follow.

Figure 1 (b) depicts TC-BGM ionization probabilities for  $\text{He}^{2+}$ -Li and  $\text{Li}^{2+}$ -Li collisions. The change in the projectile potential yields changes in ionization probabilities. The potentials for both projectiles have the same Coulomb tail, and it is only in the vicinity of the projectile (less than  $\sim 2$  a.u.) that the projectile potentials differ significantly. Therefore, the biggest changes in the probabilities ought to be observed for low values of the impact parameter. The change is more pronounced for  $1s$  ionization, due to the fact that the  $1s$  wave function is compact around the atomic center and is without a node near or at the center, unlike the  $2s$  and  $2p$  wave functions, respectively. As a result, it is inner-shell ionization that changes the most in comparison with  $\text{He}^{2+}$ -Li collisions.

Since collisions with small impact parameters are most likely to produce electrons with energies too high to be detected with the apparatus used in this work, we disregard the differences in projectile ( $\text{Li}^{2+}$  vs  $\text{He}^{2+}$ ) as irrelevant to our work and use the CDW-EIS method for  $\text{He}^{2+}$ -Li collisions henceforth to describe the  $\text{Li}^{2+}$ -Li experiments. Finally, we note that according to our TC-BGM calculations the probability for electron capture by the projectile is negligibly small, therefore it is ignored in our analysis.

### 3. Results

Figure 2 presents experimental and theoretical SDCSs for ionization from the ground and excited states of the lithium target. The theoretical SAE model SDCSs for ionization of valence electrons (triangles), for both ground and excited Li targets, are in a very good agreement with the experimental data (diamonds). The removal of the valence electron for this system can, therefore, be understood as a pure single-particle process. The perturbation is too weak for the tightly bound inner-shell electrons to participate actively in the removal of the loosely bound valence



**Figure 2.** SDCSs for electron removal in  $\text{Li}^{2+}\text{-Li}(1s^2 2s)$  (orange) and  $\text{Li}^{2+}\text{-Li}(1s^2 2p)$  (black) collisions. Diamonds: experimental SDCSs for outer-shell ionization, squares: experimental SDCSs for inner-shell ionization, triangles: SAE model SDCSs for outer-shell ionization, circles: SAE model SDCSs for inner-shell ionization, which does not distinguish between the two Li-target configurations. The theoretical results were connected by straight lines.

electron.

In the case of  $\text{Li}(1s)$  ionization we observe a big discrepancy between the SAE model CDW-EIS (circles) and the experimental (squares) results, reaching over an order of magnitude for the lowest-energy electrons removed from the excited-state Li target. This shows that the ionization of inner-shell electrons is a more complex process. To investigate this difference we follow the work presented in [7] and incorporate many-body phenomena in a way briefly discussed in the previous section.

There are many possible paths that can lead to  $1s$  vacancy production leaving the target in an ionic excited configuration. Among the most important are: (i) Exclusive ionization, where one  $1s$  electron is removed, whereas the two electrons that are left behind remain unaffected; (ii) Excitation-ionization, with one-electron removal from the inner shell, one-electron excitation from the outer shell, and the residual inner-shell electron remaining unaffected; (iii) Excitation-ionization, with one-electron removal from the outer shell, one-electron excitation from the inner shell, and the residual inner-shell electron remaining unaffected; (iv) Shake-off, here one  $1s$  electron is excited while the  $2s$  electron is shaken-off ending up in the continuum, whereas the residual inner-shell electron remains unaffected.

Moreover, we consider process (iii) as a sequential process in an independent event (IEV) model where firstly, the valence electron is removed and only after the subsequent rearrangement of the inner-shell electrons, a single  $1s$  electron gets promoted to an excited state of the lithium ion. In order to calculate probabilities for elastic scattering and excitation of a  $1s$  electron in  $\text{Li}^+$  we replace the OPM potential for  $\text{Li}(1s^2 2s)$  with the OPM potential for  $\text{Li}^+(1s^2)$ . Adjustment of the  $2s$  electron to the excited ionic state after inner-shell ionization (process (ii)) appears to be much less likely to happen. Hence, we restrict ourselves to consider only process (iii) within the IEV model.

Our last amendment to the model addresses the restricted target basis used in the TC-BGM calculations. The basis set used here allows excitations to states with principal quantum number not higher than  $n = 4$ . In our analysis we extend the number of possible excitations to exceed

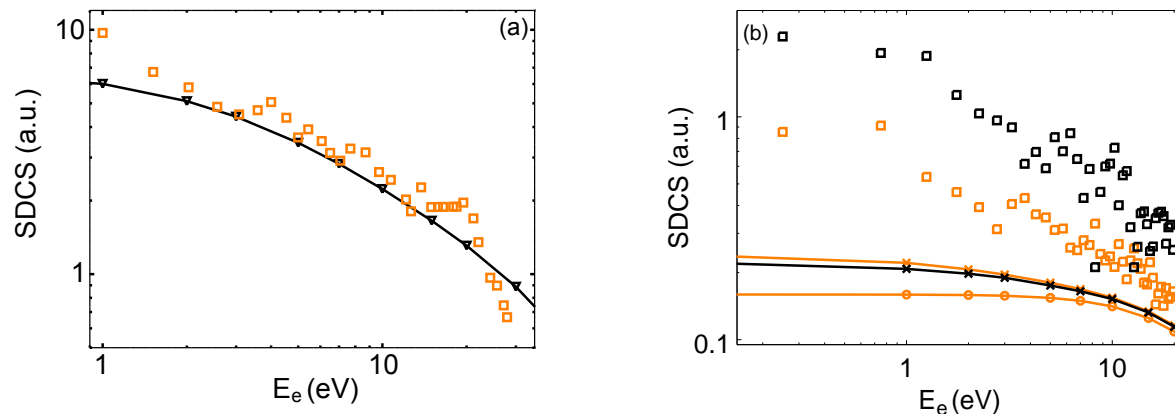


**Figure 3.** (a)  $O^{8+}$ - $Li(1s^2 2s)$  SDCS for inner-shell ionization. Theory - Triangles connected by full line (from [7]), experiment - squares (from [2]). (b) SDCSs for the inner-shell electron removal in  $Li^{2+}$ - $Li(1s^2 2s)$  (orange) and  $Li^{2+}$ - $Li(1s^2 2p)$  (black) collisions. Squares depict experimental SDCSs. Crosses depict SDCSs that take into account processes (i)-(iv), and circles depict SAE model SDCSs.

$n = 4$  in an approximate way, by assuming that they scale like  $1/n^3$  [13]. This allows us to extrapolate excitation probabilities for principal quantum number  $n \rightarrow \infty$ . The effect of the extrapolation is to provide a 10% to 50% increase in SDCSs.

Taking into account the aforementioned paths, with a leading role of the excitation-ionization process, together with incorporating the IEV model, and extrapolation of excitation probabilities, allowed Kirchner and co-workers [7] to explain successfully the experimental SDCS for  $1s$  ionization in  $O^{8+}$ - $Li(1s^2 2s)$  collisions at 1500 keV/amu (see figure 3 (a)). We perform a similar analysis to understand the experimental SDCSs for removal of a  $1s$  electron in figure 2.

Figure 3 (b) depicts experimental SDCSs for removal of a  $1s$  electron (squares) by  $Li^{2+}$  impact, together with theoretical SDCSs where processes from (i)-(iv) are accounted for (crosses) and with SAE model SDCSs (circles). It can be clearly seen that for both ground and excited states of the Li target these multi-electron processes do not contribute sufficiently to explain the experimental results. Another interesting feature is that the ground-state SDCS, in the low-energy part, has a greater magnitude than the excited-state SDCS, contrary to the experimental results. Note, that the SAE model curves fall on top of each other, since we use the same effective potential representing the interactions of ground- and excited-state configurations.

We now turn our attention to each process from (i) to (iv) separately, and to their contributions to the total multi-electron SDCSs (squares in figure 4). The exclusive ionization process (triangles in figure 4) dominates the total SDCSs for inner-shell electron removal for both ground and excited states of the target. Moreover, the resemblance with the SAE model SDCSs (see figure 3 (b)) is striking. This means that the probabilities for leaving both inner- and outer-shell electrons unaffected are close to unity, ruling out any other contribution as significant. The other contributions are indeed considerably weaker and do not constitute even 40% of the total SDCSs. These contributions are not sufficient to explain the discrepancy between theory and experiment. Note that an extra contribution to the collision with excited lithium atoms has been added (dashed line in figure 4), namely deexcitation-ionization, where the outer-shell electron gets deexcited ( $2p \rightarrow 2s$ ) while one of the inner-shell electrons is ionized.

Although the discrepancy between experimental and theoretical data is not fully understood we may speculate that a different multi-electron process (or processes) may be involved. In

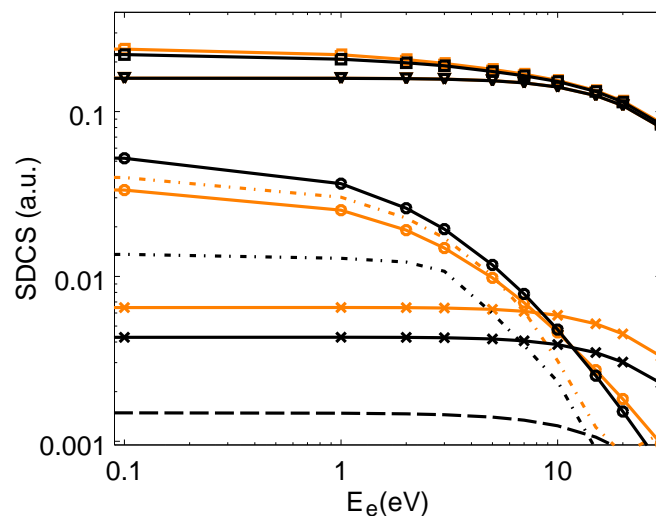


**Figure 4.** Multi-electron contributions to the total SDCSs for Li( $1s^2 2s$ ) (orange curves) and Li( $1s^2 2p$ ) (black curves) target configurations. Triangles: process (i), crosses: process (ii), circles: process (iii) in the IEV model, dashed-dotted: process (iv), dashed: deexcitation-ionization (see the text), squares: total SDCS.

particular, it could be a process that involves outer-shell ionization, as can be seen from the slopes of the experimental SDCS results. The outer-shell-ionization SDCS decreases much more rapidly with electron energy than inner-shell-ionization SDCS. Since the deficiency in the theoretical result lies in the low-energy part, it is a process with outer-shell ionization involvement that could reduce this difference, provided it is of sufficient magnitude.

One candidate is a direct interaction of the projectile electron with the valence target electron. It was shown that such an interaction may lead to simultaneous target ionization and projectile excitation or ionization [14, 15]. Theoretical estimates of these processes result in at most small contributions to the SDCS. Nevertheless, it would be interesting to look for experimental signatures of projectile electron transitions. For example, a measurement of the final projectile charge state could be used to rule out projectile ionization.

#### 4. Conclusions

We have shown that due to the strong binding of the inner-shell electrons, outer-shell ionization in  $\text{Li}^{2+}\text{-Li}(1s^2 2s)$  and  $\text{Li}^{2+}\text{-Li}(1s^2 2p)$  collisions at 2290 keV/amu is solely a one-electron process. This was also observed for collision systems with a much stronger perturbation [2].

The theoretical results for  $1s$  electron removal do not reproduce the experimental results. Moreover, the comparison has brought us to contradictory conclusions. First, the dominant contribution of  $1s$  exclusive ionization to the total SDCS and its resemblance to the SAE model SDCS suggest that the process has, at least to a high degree, a single-electron nature. Secondly, the discrepancy between the full multi-electron SDCS and the experiment indicates that a significant multi-electron process or processes involving ionization from the valence shell are missing from our analysis.

#### Acknowledgements

The theoretical portion of this work was supported by the Natural Sciences and Engineering Research Council of Canada and by the Hungarian Scientific Research Fund (OTKA Grant No.



K 109440). The experiments were funded through the Emmy-Noether program of the German Research Council (DFG), under Grant No. FI 1593/1-1 and were supported by the Alliance Program of the Helmholtz Association under Grant No. HA216/EMMI. MS acknowledges support from the National Science Foundation (Grant No. PHY-1401586).

## References

- [1] Schulz M and Madison D H 2006 *Int. J. Mod. Phys. A* **21** 3649
- [2] Fischer D, Globig D, Goullon J, Grieser M, Hubele R, de Jesus V L B, Kelkar A, LaForge A, Lindenblatt H, Misra D, Najjari B, Schneider K, Schulz M, Sell M and Wang X 2012 *Phys. Rev. Lett.* **109**(11) 113202
- [3] LaForge A C, Hubele R, Goullon J, Wang X, Schneider K, de Jesus V L B, Najjari B, Voitkiv A B, Grieser M, Schulz M and Fischer D 2013 *J. Phys. B* **46** 031001
- [4] Hubele R, LaForge A, Schulz M, Goullon J, Wang X, Najjari B, Ferreira N, Grieser M, de Jesus V L B, Moshhammer R, Schneider K, Voitkiv A B and Fischer D 2013 *Phys. Rev. Lett.* **110**(13) 133201
- [5] Ciappina M F, Pindzola M S and Colgan J 2013 *Phys. Rev. A* **87**(4) 042706
- [6] Walters H R J and Whelan C T 2014 *Phys. Rev. A* **89**(3) 032709
- [7] Kirchner T, Khazai N and Gulyás L 2014 *Phys. Rev. A* **89**(6) 062702
- [8] Hubele R, Schuricke M, Goullon J, Lindenblatt H, Ferreira N, Laforge A, Brühl E, de Jesus V L B, Globig D, Kelkar A, Misra D, Schneider K, Schulz M, Sell M, Song Z, Wang X, Zhang S and Fischer D 2014 (*Preprint arXiv:1411.0838*)
- [9] Ullrich J, Moshhammer R, Dorn A, Dörner R, Schmidt L P H and Schmidt-Böcking H 2003 *Rep. Prog. Phys.* **66** 1463
- [10] Engel E and Vosko S H 1993 *Phys. Rev. A* **47**(4) 2800–2811
- [11] Zapukhlyak M, Kirchner T, Lüdde H J, Knoop S, Morgenstern R and Hoekstra R 2005 *J. Phys. B* **38** 2353
- [12] Lüdde H J and Dreizler R M 1985 *J. Phys. B* **18** 107
- [13] Röhrbein D, Kirchner T and Fritzsche S 2010 *Phys. Rev. A* **81**(4) 042701
- [14] Dörner R, Mergel V, Ali R, Buck U, Cocks C L, Froschauer K, Jagutzki O, Lencinas S, Meyerhof W E, Nüttgens S, Olson R E, Schmidt-Böcking H, Spielberger L, Tökesi K, Ullrich J, Unverzagt M and Wu W 1994 *Phys. Rev. Lett.* **72**(20) 3166
- [15] Zhang S F, Fischer D, Schulz M, Voitkiv A B, Senftleben A, Dorn A, Ullrich J, Ma X and Moshhammer R 2014 *Phys. Rev. Lett.* **112**(2) 023201